

# Photo-Tunable Elastomers Enabling Reversible, Broad-Range Modulation of Mechanical Properties Via Dynamic Covalent Crosslinkers

Sihwan Lee, Yong Eun Cho, Ho-Young Kim,\* and Jeong-Yun Sun\*

Modulating the mechanical properties of soft materials with light is essential for achieving customizable functionalities. However, existing photo-responsive materials suffer from limited mechanical performance and a restricted tunable range. Here, a photo-tunable elastomer is developed by incorporating a urethane acrylate network with selenosulfide-based dynamic covalent crosslinkers, achieving high tensile strength exceeding 1.2 MPa in their stiff state and variable Young's modulus within a 0.8 MPa range. These crosslinkers undergo selenosulfide photo-metathesis, gradually breaking under ultraviolet light and reforming under visible light, enabling fine control over the modulus, strength, and stretchability of the elastomer. In terms of controllability, the design supports multiple tunable states, which allow for the use of intermediate mechanical properties. Moreover, by modeling the crosslinking density changes with reaction kinetics, modulus variation is predicted as a function of light exposure time. The light-induced modulation facilitates localized mechanical property adjustments, generating transformable multi-material structures and enhancing fracture resistance. Integrating these crosslinkers into different polymer networks provides a strategy for creating various photo-tunable elastomers and gels.

## 1. Introduction

Elastomers, network polymers with crosslinked structures, possess stretchability and compliance.<sup>[1]</sup> For effective utilization of these features, tailored and robust mechanical properties are essential.<sup>[2]</sup> The mechanical properties of elastomers depend on how their polymer chains are connected.<sup>[3e]</sup> Once polymerized, these connections generally cannot be changed, giving each elastomer its intrinsic mechanical properties. Their fixed mechanical properties prevent the materials from adapting to diverse environments.<sup>[4]</sup> Hence, under various conditions, achieving customizable properties requires producing different elastomers with tailored characteristics,<sup>[5]</sup> which can lead to complex processing<sup>[6]</sup> and resource waste.<sup>[7]</sup> To overcome these limitations, property tunable elastomers are gaining significant attention.

A promising strategy for property modulation involves introducing dynamic covalent bonds into network polymers, enabling the alteration of network

properties in response to stimuli.<sup>[8]</sup> Among various stimuli, light is particularly advantageous due to its directionality for patterning and its adjustable wavelength.<sup>[9]</sup> The utilization of photo-responsive dynamic covalent bonds like azobenzene,<sup>[10]</sup> coumarin,<sup>[11]</sup> spiropyran,<sup>[12]</sup> thioindigo,<sup>[13]</sup> thiol-ene,<sup>[14]</sup> and thiuram disulfide<sup>[15]</sup> enhances the ability to control network modifications, such as reversible switching. However, previous studies used solvents or flexible chains like polyethylene glycol (PEG) to assist bond conversion, which compromised both strength and stiffness. This limited mechanical integrity restricts modulation within a narrow range of mechanical properties, such as tensile strength and Young's modulus.

Here, we report a photo-tunable elastomer with a urethane acrylate network incorporating selenosulfide-based dynamic covalent crosslinkers, which facilitate drastic tuning of mechanical properties while preserving mechanical performance. This feature stems from the crosslinkers containing diselenide (DSe) units, which dynamically exchange with mobile disulfide (DS) bonds under light exposure. By utilizing selenosulfide photo-metathesis, we achieve gradual and reversible control of

S. Lee, Y. E. Cho, J.-Y. Sun  
Department of Materials Science and Engineering  
Seoul National University  
Seoul 08826, Republic of Korea  
E-mail: [jysun@snu.ac.kr](mailto:jysun@snu.ac.kr)

H.-Y. Kim, J.-Y. Sun  
Department of Mechanical Engineering  
Seoul National University  
Seoul 08826, Republic of Korea  
E-mail: [hyk@snu.ac.kr](mailto:hyk@snu.ac.kr)

J.-Y. Sun  
Research Institute of Advanced Materials (RIAM)  
Seoul National University  
Seoul 08826, Republic of Korea

 The ORCID identification number(s) for the author(s) of this article can be found under <https://doi.org/10.1002/smll.202412657>

© 2025 The Author(s). Small published by Wiley-VCH GmbH. This is an open access article under the terms of the [Creative Commons Attribution-NonCommercial](https://creativecommons.org/licenses/by-nc/4.0/) License, which permits use, distribution and reproduction in any medium, provided the original work is properly cited and is not used for commercial purposes.

DOI: 10.1002/smll.202412657

crosslinking density. The crosslinking density remains persistent even after the light is turned off, enabling multiple tunable states. Therefore, our photo-tunable elastomer offers precise and wide-range modulation of modulus, strength, and stretchability. Moreover, the light-responsive modulation allows for photopatterning, and our photo-tunable crosslinkers can be applied to various elastomers and gels.

## 2. Results and Discussion

### 2.1. Design of Photo-Tunable elastomers

As illustrated in **Figure 1A**, the photo-tunable elastomer consists of main chains, photo-tunable crosslinkers with DSe groups, and exchangers with DS groups. DSe is incorporated into the urethane acrylate crosslinker, and the urethane bonds mechanically reinforce the network (**Figure S2**, Supporting Information).<sup>[16]</sup> When combined with poly(2-hydroxyethyl acrylate) (pHEA) chains, the crosslinkers facilitate the formation of a tough elastomer. Additionally, the exchanger, which is mobile and non-volatile, ensures stable exchange reactions even in a solvent-free network. The DSe in the crosslinker and the DS in the exchanger undergo reversible photo-metathesis under ultraviolet (UV) and visible (Vis) light (**Text S2** and **Figures S3** and **S4**, Supporting Information).<sup>[17]</sup> In the network, UV light breaks the DSe crosslinks, reducing the crosslinking density, which is determined by the number of intact DSe bonds, and creating dangling ends. Vis light restores the DSe bonds, increasing the crosslinking density by forming new connections. This network topology change can be gradually controlled by adjusting the light exposure time. At high crosslinking density, the crosslink points hold the main chain under load, making the elastomer stiff. In contrast, at low crosslinking density, the main chain slips under the same load, rendering the elastomer more compliant and stretchable.

We can control the mechanical properties of our elastomers through light exposure, as clearly demonstrated in tensile tests. In the as-prepared state of the photo-tunable pHEA elastomer, the strength is 1260 kPa, and the stretchability is 2.52. Increasing UV exposure time gradually decreases the strength to 460 kPa and increases the stretchability to 3.43 (**Figure 1B**). The properties become saturated after 8 h of UV exposure, with negligible changes observed between 8 and 16 h. When Vis light is applied to the UV 8 h sample, the strength of the softened elastomer increases to 910 kPa, and its stretchability returns to 2.66 (**Figure 1C**). The mechanical properties become saturated after 16 h of Vis exposure, with insignificant changes observed up to 32 h. The ability to achieve gradual and persistent changes in mechanical properties ensures precise modulation. Moreover, the stability of the material under outdoor light, including sunlight, ensures reliable mechanical performance by avoiding unintended bond exchange. This mechanical property tuning can also be observed by measuring the elongation of the elastomer under a constant load of 120 g (**Figure 1D**). The as-prepared sample stretches to 60% of its initial length. As the UV exposure times increases, the elongation gradually becomes greater, reaching 340% after 8 h of UV exposure. When the UV-exposed sample is subsequently exposed to Vis light, it returns to its original state.

For achieving on-demand control of the photo-tunable elastomer, we used selenosulfide chemistry to enable gradual and reversible modulation under light (**Text S3** and **Figure S5**, Supporting Information). Unlike the transient behavior observed in thiol-based systems,<sup>[13–15]</sup> DSe and DS bond exchange provide persistent property adjustments, allowing for the use of intermediate states. This stability also extends to outdoor environments, where the elastomer retains its properties. The as-prepared sample exhibited no significant changes after being left outdoors for a week (**Figure S29**, Supporting Information). Additionally, the simplicity of selenosulfide chemistry facilitated the development of a robust crosslinking system, resulting in a tough elastomer. Our elastomer exhibits improved mechanical properties and a broad-range of light-driven property modulation (**Figure 1E**; **Tables S1** and **S2**, Supporting Information). A positive  $\Delta\text{Stretch}$  indicates increased stretchability after softening while maintaining toughness, whereas a negative  $\Delta\text{Stretch}$  suggests mechanical degradation following softening.

### 2.2. Bond Exchange

To evaluate changes in network topology, we examined the characteristics of the bond exchange between DSe and DS. The photo-metathesis reaction is driven by the differing absorption wavelengths of DSe, DS, and selenosulfide (SeS). DSe absorbs light from 300 nm in the UV range to 510 nm in the blue light spectrum, whereas DS absorbs only between 300 and 370 nm in the UV range (**Figure 2A**). Additionally, the mixture containing SeS, formed via UV-induced bond exchange, absorbs light from 300 to 510 nm, like DSe. Consequently, UV exposure induces random bond exchanges that increase SeS formation, while Vis light causes DS to accumulate and SeS to decrease (**Figure 2B**; **Figure S3**, Supporting Information). To analyze the bond exchange, we prepared solutions of 2-hydroxyethyl diselenide (HEDSe) and 2-hydroxyethyl disulfide (HEDS) for NMR analysis.<sup>[17a]</sup> <sup>77</sup>Se-NMR analysis reveals that UV light converts DSe (257 ppm peak) to SeS (422 ppm peak), whereas Vis light reverses this process, reducing SeS and increasing DSe (**Figure 2C**). This trend is also evident from <sup>1</sup>H-NMR data, specifically the changes in the 3.93 ppm peak and 3.11 ppm peak (**Figure 2D**). Both HEDSe and HEDS have peaks at 3.93 ppm (**Figure S8**, Supporting Information), overlapping at this point. Upon exposure to UV light, SeS formation sharpens the peak, and additional Vis exposure returns the peak to the as-prepared state. For hydrogen adjacent to DSe or DS, HEDSe has a peak at 3.11 ppm and HEDS has a peak at 2.89 ppm. The integration ratio of the 3.11 ppm peak to the 2.89 ppm peak changes under UV and Vis light, indicating the conversion of photo-metathesis.

The bond conversion was measured over time under UV and Vis exposure (**Figure 2E**). In UV-induced photo-metathesis, bond exchange occurs randomly, and it is an equilibrium reaction. Thus, if the initial concentrations of DSe and DS are equal, the conversion reaches  $\approx 50\%$ . Conversely, under Vis light, the conversion decreases, with  $\approx 5\%$  hysteresis (**Text S2** and **Figure S3**, Supporting Information). Additionally, the bond exchange under UV light is 2.5 times faster than under Vis light. Following sufficient Vis exposure, the SeS concentration drops, significantly reducing the probability of SeS molecules encountering each other.

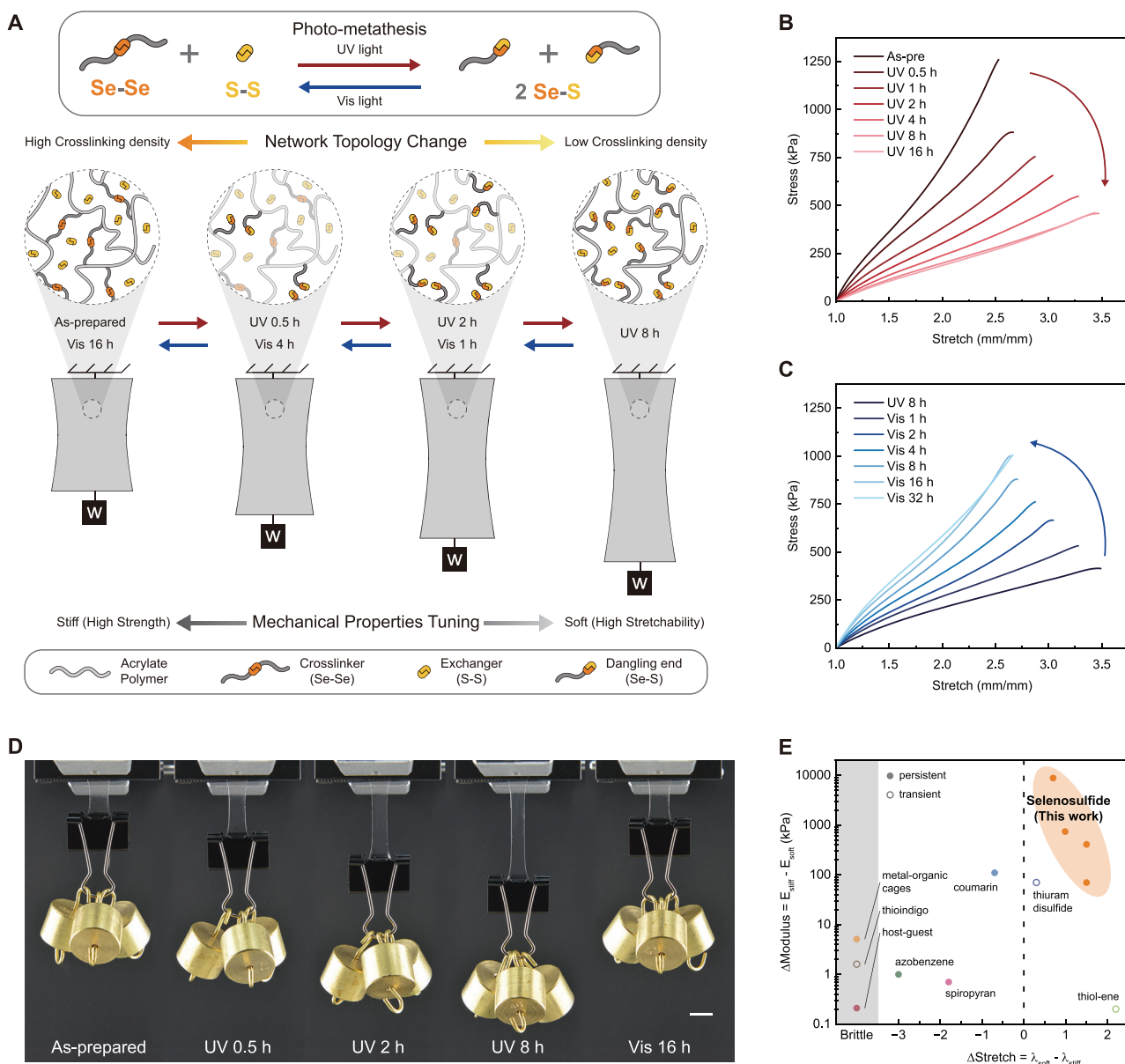


**Figure 1.** Design of photo-tunable elastomers. A) Schematic illustration of photo-tunable networks. The networks consist of polymer chains connected by photo-tunable crosslinkers that include DSe. The polymer matrix includes DS exchangers. DSe and DS engage in reversible photo-metathesis reactions triggered by UV and Vis light. Leveraging these reactions, the crosslinking density within the polymer network can be gradually modulated through light exposure, facilitating the mechanical properties tuning. B,C) Stress-stretch curves of photo-tunable pHEA elastomer showing UV softening (B) and Vis stiffening (C). For (C), each data curve was measured after a specific duration of Vis exposure following 8 h of UV exposure. D) Optical image of photo-tunable pHEA elastomers with an original width, thickness, and length of 10, 0.4, and 10 mm, respectively, under an external load of 120 g. Each sample was exposed to light individually, and the Vis 16 h sample was subjected to 8 h of UV exposure followed by 16 h of visible light exposure. The stiffness of the elastomer decreases with UV exposure and increases under Vis exposure. Scale bar, 10 mm. E) Comparison of mechanical property changes in reversibly photo-tunable materials. The x-axis represents the changes in stretch, while the y-axis represents the changes in modulus due to photo-tuning. If only rheological data were available instead of stress-stretch curves, the materials were marked in the grey area. A negative value in the stretch change indicates that the toughness is degraded when photo-tuning from a stiff to a soft state. The data used are summarized in Table S1 (Supporting Information).

Multiple reversible cycles are feasible with UV and Vis exposure (Figure 2F). Each UV cycle reaches  $\approx 50\%$  conversion, while Vis cycles revert the conversion to  $\approx 5\%$ . The reaction state is maintained when the light is turned off, allowing for pause and restart (Figure S9, Supporting Information). Even if light exposure is in-

termittent, the same conversion can be achieved when the total exposure time is equal. Increasing light intensity accelerates the reaction rate (Figure S10, Supporting Information). The reaction rate also varies with concentration (Figure 2G), with higher concentrations resulting in faster rates. If initial concentrations are

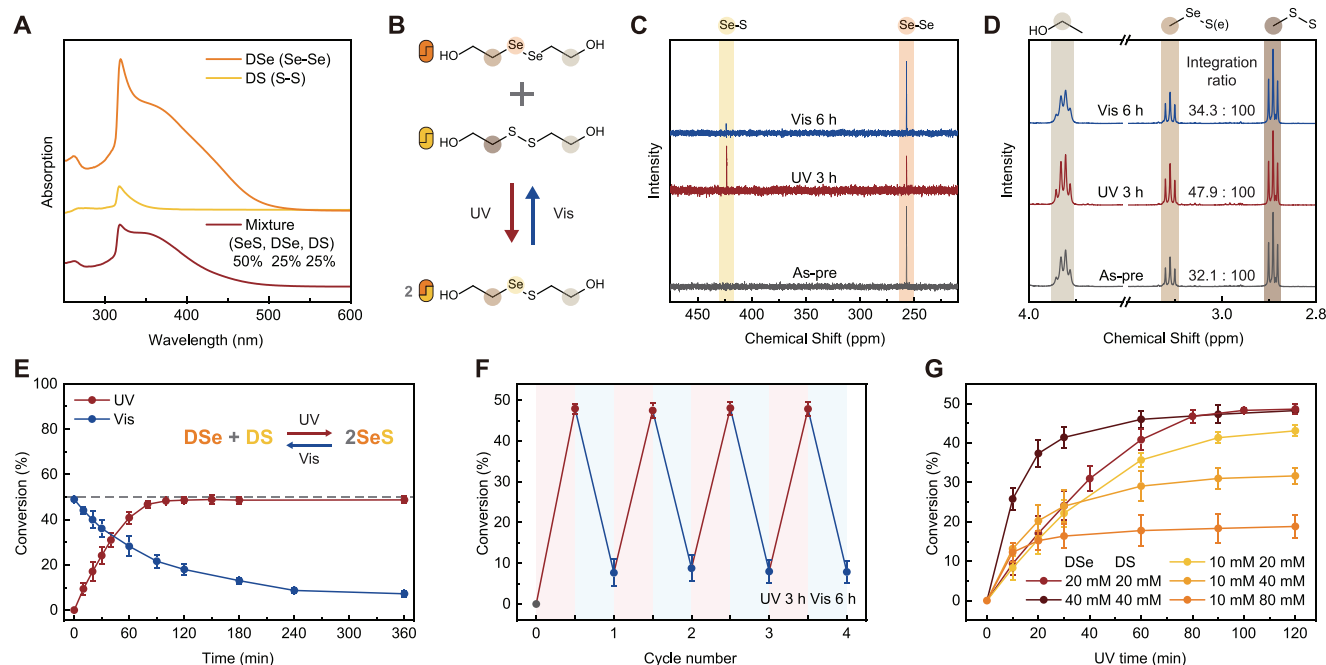


**Figure 2.** Characterizations of bond exchange. A) UV-vis absorption spectra of DSe 1 mM, DS 1 mM, and a mixture (SeS 0.5 mM + DSe 0.25 mM + DS 0.25 mM). The mixture sample was prepared by mixing DSe 0.5 mM and DS 0.5 mM and then exposing it to UV for 3 h. B) Reaction scheme illustrating the photo-metathesis between DS and DSe. C,D)  $^{77}\text{Se}$  NMR (C) and  $^1\text{H}$  NMR (D) spectra of the mixture (DSe 20 mM + DS 20 mM) before the reaction, after UV irradiation, and following recovery under Vis irradiation. E) Conversion of the bond exchange reaction versus irradiation time under UV and Vis. F) Conversion versus the number of cycles under UV and Vis irradiation. G) Conversion versus UV irradiation time at various concentrations of DSe and DS. For the Vis data in (C-F), each data was measured after a specific duration of Vis exposure following 3 h of UV exposure. Error bars denote SDs;  $n = 3$ .

the same, the saturated conversion is identical. Since UV-induced bond exchange is random, changing the initial concentration ratio modulates the equilibrium conversion depending on SeS concentration. When the initial DSe to DS concentration ratio is 1:2, it converges to 44%; at 1:4, it reaches 32%; and at 1:8, it drops to 19%. As the ratio difference increases, the equilibrium conversion decreases, but the reduction ratio of DSe relative to its initial concentration increases. Following sufficient UV exposure, the DSe concentration drops by 50% at a 1:1 ratio, but by 89% at a 1:8 ratio. The bond conversion can be precisely controlled by adjusting light exposure time, intensity, and reactant concentrations.

Bond exchange occurs within the photo-tunable network, and by predicting this process, we can anticipate changes in mechanical properties based on light exposure time (Figure 3A). To accurately predict bond exchange, it is important to account for both the reaction kinetics of photo-metathesis and the mobility within the elastomer. The reaction kinetics of photo-metathesis can be modeled by fitting the initial reaction rates ( $r$ ) at different concentrations. Under UV light, the reaction follows second-order kinetics with respect to both DSe and DS (Figure 3B).<sup>[17b]</sup> When the DSe concentration is fixed at 20 mM and the DS concentration is varied, the initial reaction rate shows a linear relationship with DS concentration. Similarly, fixing the DS concentration at 20 mM and varying the DSe concentration results in a linear relationship between the rate and DSe concentration. Therefore, the rate law is determined to be  $r = k_{UV}[DSe][DS]$ , with the rate constant ( $k_{UV}$ ) calculated to be  $0.86 \text{ M}^{-1} \text{ min}^{-1}$ .

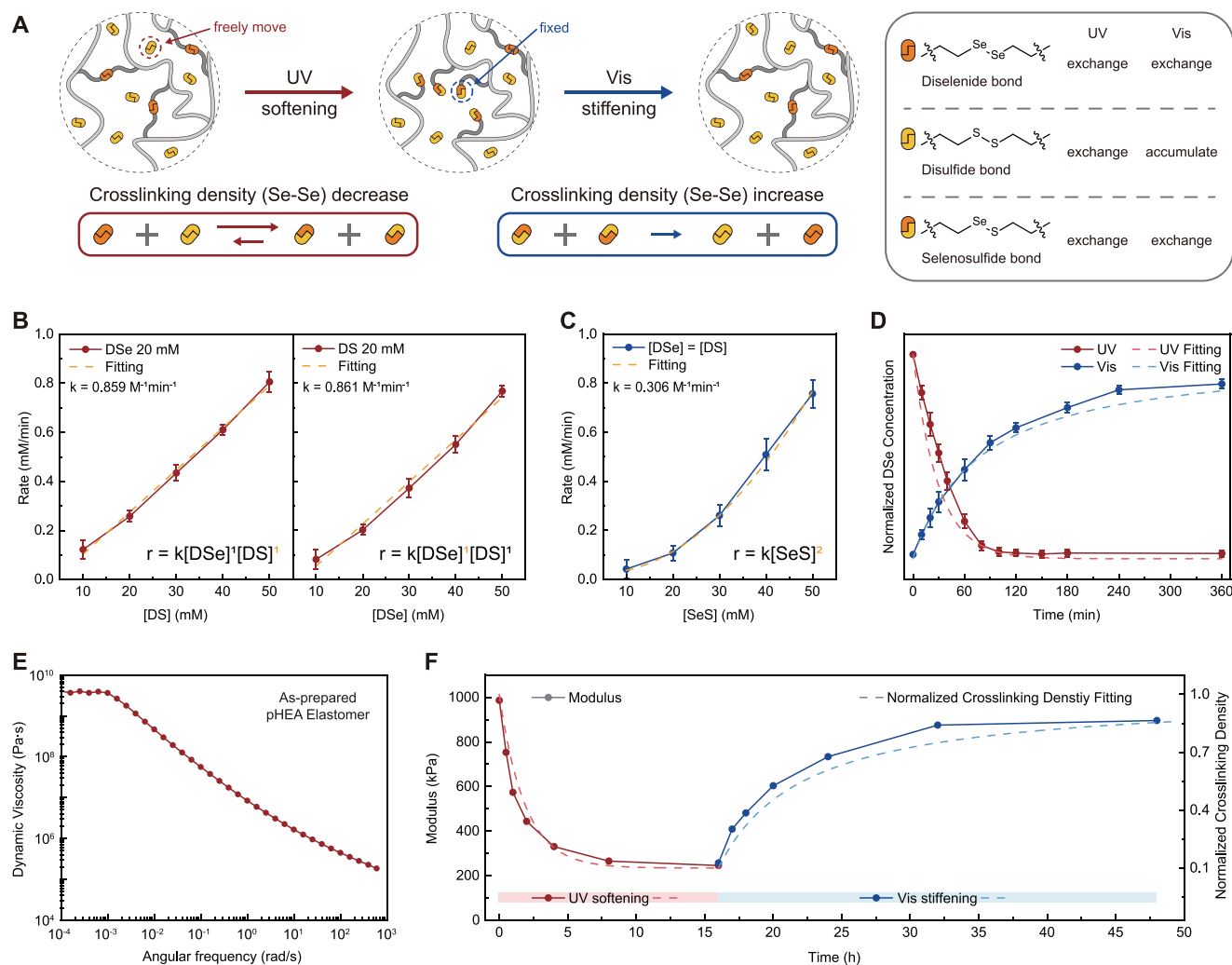
Under Vis light, the reaction follows second-order kinetics with respect to SeS (Figure 3C). The initial rate is proportional to the square of the SeS concentration, resulting in a rate law of  $r = k_{Vis}[SeS]^2$ . The rate constant  $k_{Vis}$  is calculated to be  $0.31 \text{ M}^{-1} \text{ min}^{-1}$ . Changing the intensity or wavelength of the light source modulates both  $k_{UV}$  and  $k_{Vis}$ . Based on the rate laws, we derived the concentration changes of DSe over UV exposure time ( $x_{UV}$ ) and Vis exposure time ( $x_{Vis}$ ) (Text S4, Supporting Information).

$$x_{UV} = \left( \frac{1}{[DSe]_0} + \frac{1}{[DS]_0} \right)^{-1} (1 - \exp(-k_{UV}([DSe]_0 + [DS]_0)t_{UV})) \quad (1)$$

$$x_{Vis} = \frac{2[SeS]_{UV, \infty}^2 k_{Vis} t_{Vis}}{2[SeS]_{UV, \infty} k_{Vis} t_{Vis} + 1} \quad (2)$$

With the initial concentrations and rate constants, the concentration of DSe over irradiation time can be calculated using Equations (1) and (2) (Figure 3D).<sup>[18]</sup>

As the photo-tunable crosslinker contains DSe, determining the concentration of DSe in the network allows us to anticipate the mechanical properties of the elastomer. Unlike bond exchange in solution, the softening or stiffening in the polymer network takes longer due to the need to consider diffusion within the network (Figure S11, Supporting Information).<sup>[19]</sup> To reduce exchange time and enhance the photo-tuning effect, the polymer should contain more exchangers with DS than crosslinkers with DSe (Figure S27, Supporting Information). As shown in



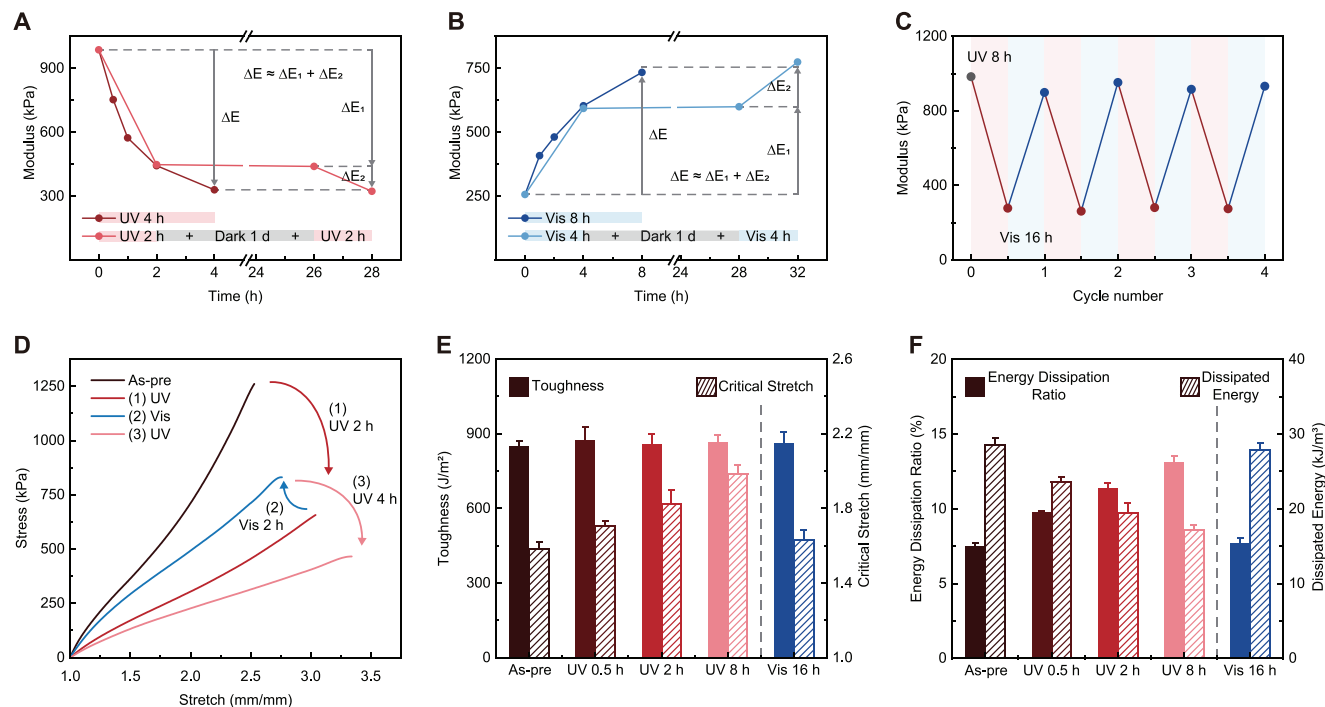
**Figure 3.** Modeling of network topology change. A) Schematic illustration of the photo-metathesis in the photo-tunable network. Under UV irradiation, the exchange reaction between DSe and DS decreases DSe bonds, reducing the crosslinking density of the polymer network. Under Vis irradiation, DS does not react and accumulates, allowing DSe bonds to reform, which increases the crosslinking density. B) Reaction kinetics of the forward reaction under UV exposure. The initial reaction rate follows second-order kinetics with respect to the concentration of DS and DSe. C) Reaction kinetics of the reverse reaction under Vis exposure. The initial reaction rate follows second-order kinetics with respect to the concentration of SeS. D) Normalized concentration of DSe versus exposure time under UV and Vis. The dashed line represents the theoretical prediction based on the rate constant. E) Dynamic viscosity of as-prepared pHEA elastomer. F) Comparison of modulus and predicted crosslinking density in response to UV and Vis exposure. The modulus was plotted based on Figure 1B,C. The normalized crosslinking density was fitted using rate constants derived from reaction kinetics and dynamic viscosity measurements.

Figure 2G, the greater the amount of DS relative to DSe, the larger the decrease in DSe concentration under UV exposure. This ratio difference also enables faster photo-tuning. Therefore, in the photo-tunable elastomer, the amount of exchanger is nine times higher than the crosslinker, based on mol% (Table S3, Supporting Information). Faster photo-tuning and a higher photo-tuning ratio can be achieved by increasing the exchanger amount, with some trade-off in mechanical properties (Figure S27, Supporting Information). However, increasing light intensity does not accelerate the bond exchange within the elastomer due to the diffusion effect (Figure S12, Supporting Information). To analyze bond exchange within the elastomer, we considered different initial concentrations of DSe and DS, as well as diffusion (Text S5, Supporting Information). To account for diffusion, we measured

the dynamic viscosity ( $\eta$ ) of the elastomer and used the Stokes-Einstein relation to determine the diffusion rate constant ( $k_{diff}$ ) (Figure 3E). By incorporating  $k_{diff}$  with  $k_{UV}$  or  $k_{Vis}$ , we account for molecular mobility within the elastomer, and the effective rate constant ( $k_{eff}$ ) is given by

$$k_{eff} = \left( \frac{1}{k_{diff}} + \frac{1}{k_{act}} \right)^{-1} \quad (3)$$

where  $k_{act}$  is the activation rate constant, equivalent to  $k_{UV}$  or  $k_{Vis}$ . By substituting  $k_{eff}$  into the rate constants in Equation (1) and (2), we can predict crosslinking density changes based on light exposure time (Figure 3F). Crosslinking density, which



**Figure 4.** Light-controlled mechanical properties of photo-tunable elastomer. A,B) Modulus-time curves showing UV softening (A) and Vis stiffening (B). When the total exposure time to UV and Vis light is equal, the modulus is almost the same. C) Young's modulus versus the number of cycles under UV and Vis irradiation. D) Stress-stretch curves of photo-tunable pHEA elastomer under alternating UV and Vis irradiation. This alternating light exposure accurately reflects the mechanical properties according to the given exposure. E) Toughness and critical stretch as influenced by UV exposure and subsequent recovery under Vis exposure. F) Hysteresis data showing energy dissipation ratio and dissipated energy with respect to UV exposure and subsequent recovery under Vis exposure. Error bars denote SDs;  $n = 3$ .

corresponds to the fraction of connected DSe bonds in the network, is fitted to predict the modulus changes in the photo-tunable elastomer. This fitting also allows for the estimation of the required light exposure time to achieve the desired mechanical properties. The correlation effectively demonstrates the relationship between nanoscale bond exchange and macroscopic mechanical property modulation.

### 2.3. Mechanical Properties Tuning

We can control the mechanical properties of our elastomers through modulating bond exchange, which has fine controllability. As shown in Figure 3F, the modulus of the photo-tunable elastomer decreases from 980 to 260 kPa under UV exposure, and then recovers to 900 kPa with Vis exposure. Mechanical property control is not only reversible and gradual, but it also exhibits consistent changes when the total exposure time is the same. The mechanical properties, such as modulus ( $E$ ), remain similar regardless of whether the light exposure is continuous or involves pausing and restarting ( $\Delta E \approx \Delta E_1 + \Delta E_2$ ). This feature, resulting from the photo-metathesis reaction, causes bond exchange to stop when light exposure is halted, leading to persistent properties (Figure S9, Supporting Information). When light exposure resumes, bond exchange starts again, modulating the properties. A sample that received UV light for 2 h, then rested in the dark for a day and received another 2 h of UV light (UV 2 h + Dark 1 d + UV 2 h) has mechanical properties comparable to a sam-

ple that received 4 h of continuous UV light (UV 4 h) (Figure 4A; Figure S13A, Supporting Information). Similarly, a sample with Vis 4 h + Dark 1 d + Vis 4 h shows a similar modulus to that of a Vis 8 h sample (Figure 4B; Figure S13B, Supporting Information). This behavior is reversible and consistent over multiple cycles (Figure 4C; Figure S14, Supporting Information). Furthermore, alternating UV and Vis light exposure fully reflects changes in mechanical properties (Figure 4D). For instance, exposing a UV 2 h sample to Vis light for 2 h increases the strength from 657 to 830 kPa and decreases the stretchability from 3.04 to 2.76. Additional UV exposure for 4 h further reduces the strength to 465 kPa and increases the stretchability to 3.34, demonstrating softening.

In addition to the stress-stretch curve, the mechanical properties of the elastomer can also be analyzed in terms of rheological, fracture, and hysteresis characteristics. In situ measurements using a photo-rheometer show that the storage modulus ( $G'$ ) decreases from 300 to 65 kPa, and the loss modulus ( $G''$ ) decreases from 46 to 20 kPa (Figure S15, Supporting Information). These changes are consistent with results obtained from samples exposed to light and measured using a standard rheometer (Figure S16, Supporting Information). This consistency indicates that mechanical properties remain stable when light exposure is halted. The decrease is more pronounced for  $G'$ , indicating an increase in damping properties of the elastomer under UV exposure. Fracture tests reveal that the toughness ( $\Gamma$ ) remains  $\approx 880 \text{ J m}^{-2}$  regardless of light exposure time (Figure 4E). Although UV exposure reduces the strength, the

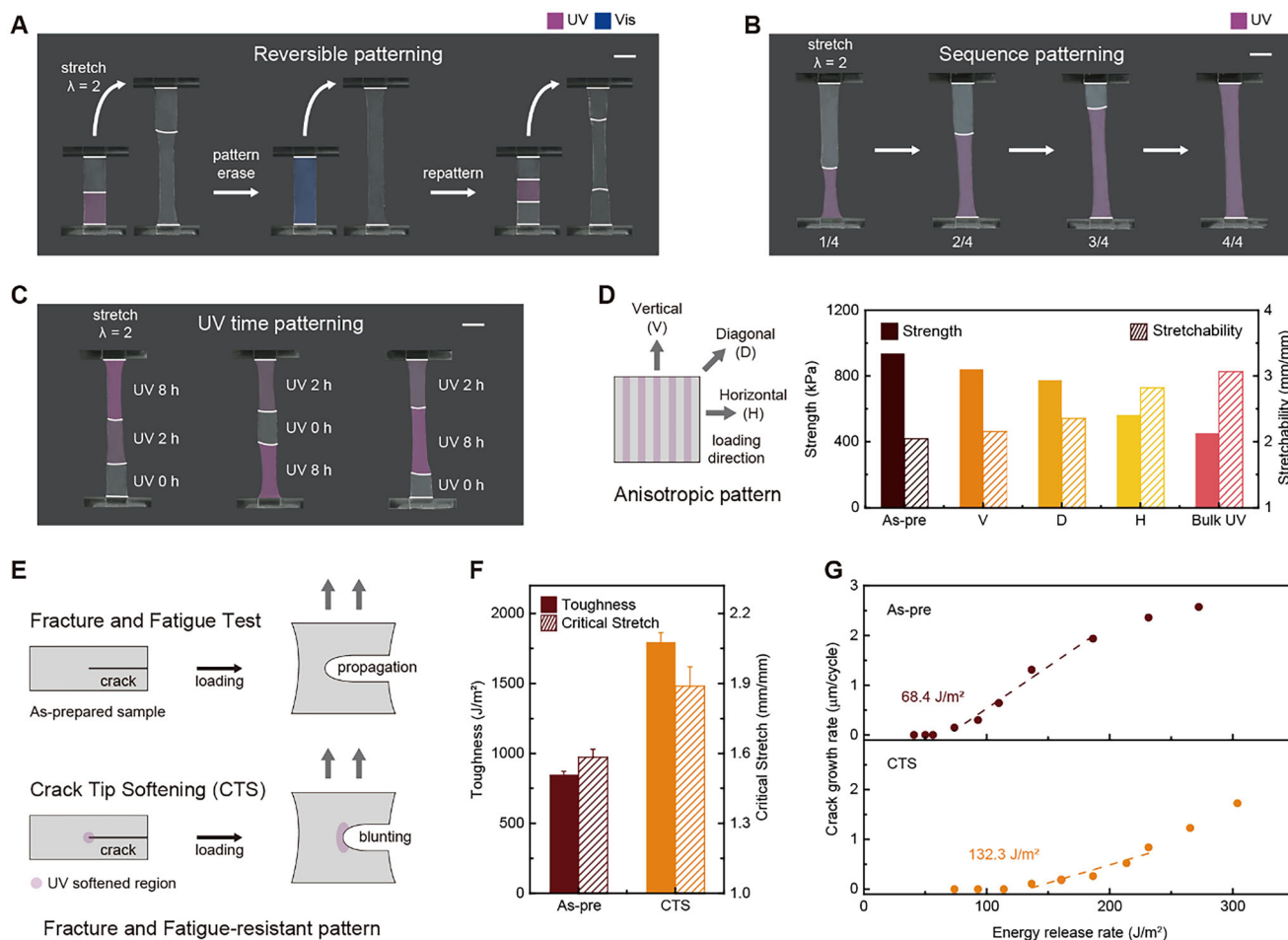


**Figure 5.** Photopatterning for mechanical metamaterials. A–C) Optical image of photopatterning in the photo-tunable pHEA elastomers. UV exposure (8 h) creates a pattern that stretches more than the unexposed region. (A) Each pattern can be erased with Vis (16 h) and repatterned using UV. (B) After UV softening, the mechanical properties can be persistently maintained, allowing for sequence patterning. (C) Gradual adjustment of UV exposure time enables different regions to exhibit distinct mechanical properties. Scale bars, 10 mm. D) Anisotropic pattern exhibits mechanical properties that vary depending on the loading direction. Strength and stretchability comparison of as-prepared, bulk UV-treated, and anisotropically patterned pHEA elastomer subjected to vertical, diagonal, and horizontal loading. The bulk UV-treated and anisotropically patterned samples were exposed to 8 h of UV irradiation. E) Schematic illustration of fracture and fatigue tests on as-prepared and CTS samples. The crack tip is blunted in CTS samples. F) Toughness and critical stretch are enhanced in the CTS samples. G) Crack growth rate versus energy release rate for as-prepared and CTS samples. The fatigue threshold is marked at the intersection of the dashed line with the point where the crack growth rate is zero.

critical stretch ( $\lambda_c$ ) increases from 1.58 to 1.98 (Figure S17 and Movie S1, Supporting Information). With sufficient Vis exposure, the strength returns to its as-prepared state, and  $\lambda_c$  decreases back to 1.62. Hysteresis data show that the energy dissipation ratio stays below 15%, increasing from 7.5% to 13.1% with UV exposure time (Figure 4F). While decreasing crosslinking density slightly increases damping properties, the elastomer remains generally elastic. This characteristic is maintained not only in the first cycle but also over ten loading-unloading cycles (Figure S18, Supporting Information). Upon exposure to Vis light, the energy dissipation ratio decreases back to  $\approx 7.7\%$ , similar to the as-prepared sample. The dissipated energy ( $W_D$ ) shows an opposite trend due to the influence of strength.<sup>[20]</sup> Despite changes in network topology affecting strength and stretchability, there is no degradation in fracture and elastic performance.

## 2.4. Photopatterning

Mechanical properties in the photo-tunable elastomer can be selectively modified through light patterning, which uses light to create localized mechanical property changes. Using UV light and a photomask, specific areas of the sample undergo UV-induced softening (Figure S19, Supporting Information).<sup>[21]</sup> This localized modulation is evident in the mechanical response under tensile stress and highlights the material's ability to generate dynamic, functional patterns. When the purple-colored half of the sample is exposed to UV and the entire sample is stretched to twice its original length, the unexposed part elongates by 23%, while the UV exposed part elongates by 173% (Figure 5A). This process is reversible, as Vis light can erase the pattern and enables repatterning. When only the middle third of the sample is exposed to UV during repatterning, the central area

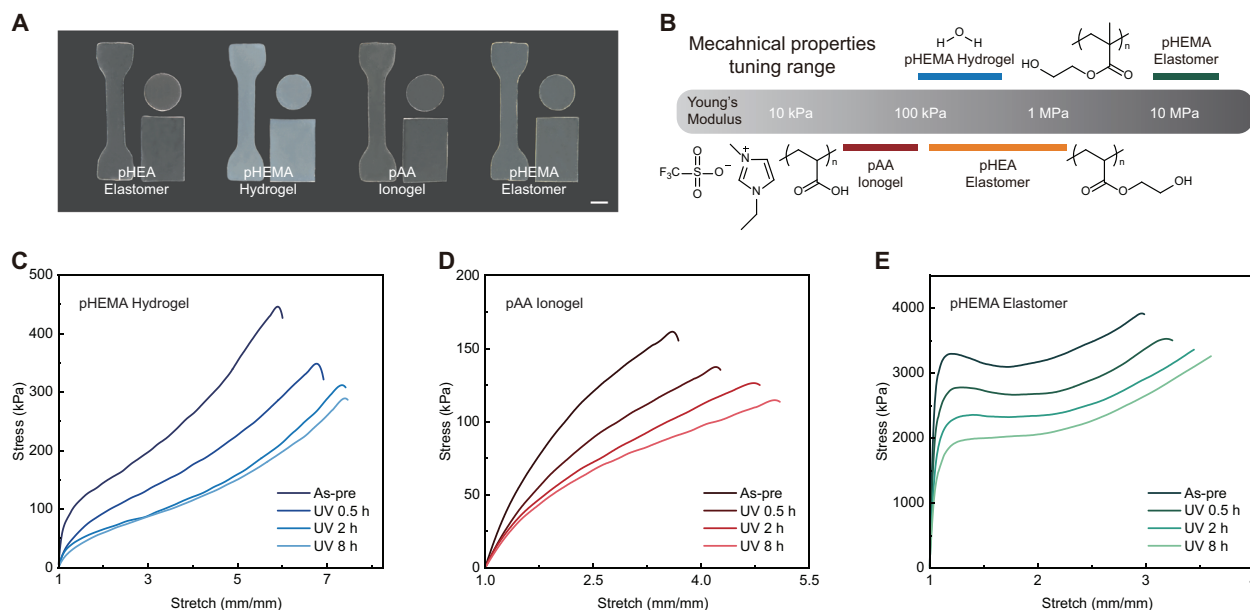


**Figure 6.** Versatility of photo-tunable crosslinker. A) Optical images of various photo-tunable elastomers and gels polymerized with the same DS crosslinker and DS exchanger: pHEA elastomer, pHEMA hydrogel, pAA ionogel, and pHEMA elastomer. Dog bone shapes are for tensile tests, circles for rheology tests, and rectangles for fracture tests. Scale bar, 5 mm. B) Young's modulus tuning range for various photo-tunable elastomers and gels. C–E) Stress-stretch curves demonstrating gradual UV softening for pHEMA hydrogel (C), pAA ionogel (D), and pHEMA elastomer (E).

elongates by 215%, while the edges elongate by only 41%. Since the transparency of the elastomer remains unchanged, only the mechanical properties are patterned (Figure S24, Supporting Information). In addition to reversible patterning, the ability to persistently maintain properties allows for sequence patterning (Figure 5B). After initial patterning, the pattern can be modified by re-exposing different areas to UV, and once the entire area is treated, the stretchability becomes uniform. Moreover, the gradual control of stretchability enables different regions of the elastomer to be patterned with varying UV exposure times (Figure 5C). Applying different UV exposure times within a single sample results in distinct stretchability across regions. A stripe UV pattern induces anisotropic properties in the elastomer, resulting in varying strength and stretchability depending on the loading direction (Figure 5D). Vertical loading shows a strength of 841 kPa and stretchability of 2.15, whereas horizontal loading is softer with a strength of 562 kPa and stretchability of 2.82. This anisotropy can be advantageous in applications requiring directional mechanical responses. Additionally, softening the area around a notch with UV light creates a blunting effect at the crack tip (Figure 5E).<sup>[22]</sup> The softened area around the crack dissipates the stress concentration. This fracture-resistant pattern increases  $\lambda_c$  from 1.6 to 1.9, thereby enhancing  $\Gamma$  from 848 to 1797 J m<sup>-2</sup> (Figure 5F; Figure S20, Supporting Information). The fatigue threshold also increased from 68.4 to 132.3 J m<sup>-2</sup> (Figure 5G; Movie S2, Supporting Information).<sup>[23]</sup>

## 2.5. Versatility

The photo-tunable crosslinkers we used to achieve the photo-tuning property can be applied to various polymeric materials

(Figure 6A).<sup>[24]</sup> By changing the type of main chain or adding solvents to form gels, the modulus can be photo-tuned across a wide-range (Figure 6B). The pHEA elastomer discussed in Figure 4 can have its modulus adjusted from 260 to 980 kPa with light exposure. The poly(2-hydroxyethyl methacrylate) (pHEMA) elastomer, which is stiffer, can be tuned from 11 to 20 MPa in modulus, while the pHEMA hydrogel with solvent can be adjusted from 150 to 560 kPa, and the poly(acrylic acid) (pAA) ionogel from 80 to 150 kPa. In addition to modulus changes, the stress-stretch curves of pHEMA hydrogel, pAA ionogel, and pHEMA elastomer differ from those of the pHEA elastomer (Figure 6C–E). All these materials can be gradually tuned with light exposure and restored with Vis light (Figure S21, Supporting Information). In gels, the presence of solvents in the polymer network accelerates photo-tuning, enabling a faster modulation to the completely soft state compared to elastomers (Figure S22, Supporting Information). By modulating the main chain polymer, a diverse range of photo-tunable elastomers and gels with various properties can be created.

## 3. Conclusion

We developed a photo-tunable elastomer that enables on-demand and wide-range modulation of mechanical properties. The control of mechanical properties allows for gradual and reversible tuning, achieved through selenosulfide photo-metathesis. The bond exchange can be precisely modeled using reaction kinetics, and the corresponding changes in crosslinking density align closely with the observed modulus variation in the elastomer. Notably, our crosslinker-based approach significantly improves both mechanical performance and the modulation range, with tensile strength ranging from 1260 to 460 kPa and stretchability

varying from 2.52 to 3.43. The modulation does not degrade fracture and elastic properties, maintaining toughness at  $\approx 880 \text{ J m}^{-2}$  and keeping the energy dissipation ratio below 15%. Furthermore, light control of the polymer network facilitates localized tuning of mechanical properties, creating transmutable multi-material structures. For example, softening around the crack tip can double both the toughness and fatigue threshold compared to the as-prepared state. Ultimately, our strategy offers the versatility to introduce crosslinkers into various network polymers, allowing the material to retain its mechanical performance while gaining photo-tunable properties. This versatility enables the development of highly adaptable photo-tunable materials, which can simplify the manufacturing process and promote resource efficiency, thereby expanding the potential applications of soft materials.

## 4. Experimental Section

**Materials:** All reagents were used as received unless otherwise stated. Selenium (Se, 99.99%), 2-Bromoethanol (BrEtOH, 95%), 2-Hydroxyethyl methacrylate (HEMA, 97%), Acrylic acid (AA, 99%), Aluminum oxide ( $\text{Al}_2\text{O}_3$ ), Hydroquinone (HQ, >99.8%), Silica gel ( $\text{SiO}_2$ ), 2-Hydroxyethyl disulfide (HEDS), Dibutyltin dilaurate (DBTDL, 95%), 1-Ethyl-3-methylimidazolium trifluoromethanesulfonate (EMIM Otf, 97%), and Chloroform-d ( $\text{CDCl}_3$ , 99.8%) were purchased from Sigma-Aldrich. Sodium Borohydride ( $\text{NaBH}_4$ , 95%), Dicyclohexylmethane 4, 4-diisocyanate (HMDI, >90%), 2-Hydroxyethyl acrylate (HEA, >95%), and Phenylbis (2, 4, 6-trimethylbenzoyl) phosphine Oxide (BAPO, >96%) were purchased from TCI chemicals. Dimethyl selenide ( $\text{Me}_2\text{Se}$ ) was purchased from Alfa Aesar. Tetrahydrofuran (THF, >99.9%), Dichloromethane (DCM, >99.8%), Ethyl acetate (EtOAc, >99.5%), N, N-dimethylformamide (DMF, 99.8%), Acetone, and Magnesium sulfate ( $\text{MgSO}_4$ ) were purchased from Sigma-Aldrich or Daejung Industry. THF and DMF were dried using 4 Å molecular sieves before use. HEA, HEMA, and AA monomers were passed through a basic alumina column before use.

**Sample Preparation:** HEA monomer and photo-tunable crosslinker (1 mol% relative to the monomer) were mixed for a day at 50 °C. BAPO initiator (0.8 wt.% relative to the monomer) was added to the monomer solution and stirred for 30 min at room temperature (RT). After  $\text{N}_2$  blowing for 1 min, the solution was degassed using a sonicator (CPX5800H-E, Emerson). Polymerization was carried out under 365 nm UV irradiation (CL-1000L, UVP) for 11 min in a glove box. The cured sample was soaked in a mixture of exchanger and acetone (1:8 wt.%) for one day. Acetone was dried at RT for two days. For the pHEMA elastomer, only the monomer was changed to HEMA and proceeded in the same manner. In the case of pHEMA hydrogel, water was used instead of acetone in the soaking process. In the case of pAA ionogel, the monomer was changed to AA, and EMIM Otf (100 wt.% relative to the monomer) was added to the solution. During the soaking process, a mixture of exchanger, acetone, and EMIM Otf (1:1:1 wt.%) was used, and acetone was dried at RT for two days.

**Glovebox:** A glove box (1730P, iNexus) under a nitrogen atmosphere was used for chemical synthesis and polymerization. Oxygen levels were kept below 0.1 ppm and water below 1 ppm, as monitored using an oxygen analyzer and a moisture sensor (Gox100, iNexus). Antechambers for sample transfer used a rotary vane pump (W2V10, WSA).

**UV-Vis Absorption Spectroscopy:** UV-Vis absorption spectra were acquired by UV-Vis spectroscopy (V-770, Jasco). The spectrometer measured in the range from 190–600 nm, with a measurement speed of 400 nm  $\text{min}^{-1}$ . Each sample was measured at a concentration of 1 mM in DMF using a quartz cuvette (KA1937, Kartell).

**Nuclear Magnetic Resonance (NMR) Spectroscopy:**  $^1\text{H}$  NMR,  $^{13}\text{C}$  NMR, and  $^{77}\text{Se}$  NMR spectra were collected on a 600 MHz NMR spectrometer

(Avance III-600, Bruker) installed at the National Center for Inter-university Research Facilities (NCIRF) at Seoul National University. Each sample was dissolved in  $\text{CDCl}_3$  for measurement. The 0 ppm reference for  $^1\text{H}$  NMR was set using Tetramethylsilane (TMS), and the chemical shift of  $\text{CDCl}_3$  was 7.26 ppm. The Chemical shift of  $\text{CDCl}_3$  in  $^{13}\text{C}$  NMR was 77.16 ppm. The 0 ppm reference for  $^{77}\text{Se}$  NMR was set using  $\text{Me}_2\text{Se}$ . Bond conversion and reaction rate measurements were performed using a 400 MHz NMR spectrometer (Avance III-400, Bruker).

**Fourier Transform Infrared (FT-IR) Spectroscopy:** FT-IR spectra were acquired by FT-IR spectroscopy (Nicolet iS50, Thermo Fisher Scientific). All data were measured in Attenuated Total Internal Reflection (ATR) mode. Urethane reaction and monomer conversion were confirmed by the FT-IR spectra.

**UV and Vis Irradiation:** The light used for UV bond exchange or UV-induced softening was 365 nm UV (CL-1000L, UVP) with an intensity of  $\approx 10 \text{ mW cm}^{-2}$ . For Vis-induced bond exchange or stiffening, the light was a 450 nm blue LED (Tube 450 nm blue, Yoonlight) with an intensity of  $\approx 220 \text{ mW cm}^{-2}$ . High-intensity UV data and photo-rheometer measurements were conducted with 365 nm UV (BW 200 V3, Dymax) with an intensity of  $\approx 1.7 \text{ W cm}^{-2}$ . The above intensities were measured with the light source positioned as close as possible to the measuring equipment, whereas in actual experiments, the sample was placed  $\approx 10 \text{ cm}$  away from the light source. For example, during Vis-induced stiffening experiments, the actual light intensity received by the sample was  $\approx 90 \text{ mW cm}^{-2}$ . The high intensity UV equipment had a point light source with a diameter of either 1 or 10 mm. All irradiations were carried out in a darkroom.

**Transmittance Measurements:** Transmittance spectra were acquired by a spectrometer (Flame-s, Ocean Optics). Measurements were taken in a darkroom using white light (Propad30, Prodean). The reference was set using a glass plate, and the samples were attached to the glass plate for measurement. The lighting equipment, glass plate, and measuring devices were fixed during the measurements. The thickness of all measured samples was 0.4 mm.

**Tensile Tests:** Tensile test was carried out using a universal testing machine (Instron 3343) equipped with a 50 kN load cell. Samples were laser cut (VLS3.5, Universal laser system) into the shape specified by ASTM Standard D-1708 (5 mm width, 20 mm gauge length). The thickness of all measured samples was 0.4 mm, and they were all gripped while attached to acrylic sheets. The stretch rates were kept constant at 4  $\text{min}^{-1}$ . The modulus was measured from the initial slope of the stress-stretch curve. Tensile loading-unloading tests were conducted with the same sample shape and stretch rate as the tensile test, with an applied stretch of 2.

**Fracture and Fatigue Tests:** Fracture test was conducted with samples in a rectangular shape (20 mm width, 5 mm gauge length). The thickness of the samples and the gripping method were the same as those used in the tensile tests. Notched samples were half-notched, and the critical stretch at which crack propagation began was determined. The stress-stretch curve was obtained using unnotched samples, and toughness was calculated by integrating up to the critical stretch. The stretch rates were kept constant at 4  $\text{min}^{-1}$ . For measuring the fatigue threshold, samples were prepared in the same manner as for the fracture tests. The loading-unloading rates were kept constant at 0.5 Hz. Crack propagation was monitored with a camcorder (HDR-CX405, Sony), and the crack growth length per cycle was estimated based on the videos. For samples that did not show observable crack propagation, at least five thousand cycles were applied. The energy release rate was calculated by integrating the unnotched stress-stretch curve.

**Rheology:** The storage and loss modulus were measured using a rheometer (DHR-2, TA Instruments). The diameter of the top stage was 20 mm, and the thickness of the sample was 0.4 mm. The samples were laser cut into circles with a diameter of 20 mm. The applied axial force was  $\approx 1 \text{ N}$ . A strain sweep was performed to determine the linear viscoelastic region (LVER), which was then used to set the strain for a frequency sweep. During the frequency sweep, a strain of 0.5% was applied, and measurements were taken over a frequency range of 0.1–100  $\text{rad s}^{-1}$ . For dynamic viscosity measurements, the same conditions were maintained,

but the frequency range was extended from 0.0001 to 600 rad s<sup>-1</sup>. For photo-rheometer measurements, an acrylic sheet structure was placed on the bottom stage, and the high-intensity UV source was connected to it. The tip diameter of the UV source was 10 mm, and the tip was positioned to ensure a UV irradiation area of 20 mm. A glass plate was placed on the acrylic sheet structure, and the sample was positioned on top of the glass plate. During measurements, applied strain and frequency were 0.5% and 0.5 rad s<sup>-1</sup>, respectively. All other conditions were kept the same.

## Supporting Information

Supporting Information is available from the Wiley Online Library or from the author.

## Acknowledgements

This work was supported by the National Research Foundation of Korea (NRF) grants funded by the Korean Government (RS-2024-00459269 and 2021-017476). The Institute of Engineering Research at Seoul National University provided research facilities for this work.

## Conflict of Interest

The authors declare no conflict of interest.

## Author Contributions

S.L. conceived the idea. S.L., H.-Y.K., and J.-Y.S. designed the research. H.-Y.K. and J.-Y.S. supervised the project. S.L. conducted the experiments. S.L., H.-Y.K., and J.-Y.S. wrote the manuscript. S.L. and Y.E.C. participated in optimizing the figures and assisted with material fabrication and characterization. All the authors contributed to the analysis and discussion of the data.

## Data Availability Statement

The data that support the findings of this study are available from the corresponding author upon reasonable request.

## Keywords

crosslinker, elastomer, mechanical property modulation, photo-tuning, selenosulfide, urethane acrylate

Received: January 20, 2025  
Revised: March 21, 2025  
Published online: April 24, 2025

- [1] L. G. Treloar, *The physics of rubber elasticity*, Oxford Univ. Press, Oxford, UK **1975**.  
[2] a) J. Steck, J. Kim, Y. Kutsovsky, Z. Suo, *Nature* **2023**, 624, 303; b) J. Y. Sun, X. H. Zhao, W. R. K. Illeperuma, O. Chaudhuri, K. H. Oh, D. J. Mooney, J. J. Vlassak, Z. G. Suo, *Nature* **2012**, 489, 133; c) J. Kim, G. Zhang, M. Shi, Z. Suo, *Science* **2021**, 374, 212; d) P. P. Hu, J. Madsen, A. L. Skov, *Nat. Commun.* **2022**, 13, 370; e) M. X. Wang, P. Y. Zhang, M. Shamsi, J. L. Thelen, W. Qian, V. K. Truong, J. Ma, J. Hu, M. D. Dickey, *Nat. Mater.* **2022**, 21, 359.

- [3] a) Y. W. Gu, J. L. Zhao, J. A. Johnson, *Angew. Chem., Int. Ed.* **2020**, 59, 5022; b) M. Vatankhah-Varnosfaderani, W. F. M. Daniel, M. H. Everhart, A. A. Pandya, H. Y. Liang, K. Matyjaszewski, A. V. Dobrynin, S. S. Sheiko, *Nature* **2017**, 549, 497; c) A. V. Dobrynin, Y. Tian, M. Jacobs, E. A. Nikitina, D. A. Ivanov, M. Maw, F. Vashahi, S. S. Sheiko, *Nat. Mater.* **2023**, 22, 1394; d) M. J. Zhong, R. Wang, K. Kawamoto, B. D. Olsen, J. A. Johnson, *Science* **2016**, 353, 1264; e) Y. E. Cho, S. Lee, S. J. Ma, J. Y. Sun, *Soft Matter* **2025**, 21, 1603.  
[4] N. R. Boynton, J. M. Dennis, N. D. Dolinski, C. A. Lindberg, A. P. Kotula, G. L. Grocke, S. L. Vivod, J. L. Lenhart, S. N. Patel, S. J. Rowan, *Science* **2024**, 383, 545.  
[5] a) H. Yuk, T. Zhang, G. A. Parada, X. Y. Liu, X. H. Zhao, *Nat. Commun.* **2016**, 7, 12028; b) M. Kim, S. Hong, J. J. Park, Y. Jung, S. H. Choi, C. Cho, I. Ha, P. Won, C. Majidi, S. H. Ko, *Adv. Mater.* **2024**, 36, 2313344; c) Y. Shao, J. Yan, Y. Zhi, C. Li, Q. Li, K. Wang, R. Xia, X. Xiang, L. Liu, G. Chen, H. Zhang, D. Cai, H. Wang, X. Cheng, C. Yang, F. Ren, Y. Yu, *Nat. Commun.* **2024**, 15, 6106.  
[6] a) M. A. Skylar-Scott, J. Mueller, C. W. Visser, J. A. Lewis, *Nature* **2019**, 575, 330; b) X. Kuang, J. T. Wu, K. J. Chen, Z. Zhao, Z. Ding, F. J. Y. Hu, D. N. Fang, H. J. Qi, *Sci. Adv.* **2019**, 5, aav5790.  
[7] S. Kamarulzaman, Z. M. Png, E. Q. Lim, I. Z. S. Lim, Z. B. Li, S. S. Goh, *Chem* **2023**, 9, 2771.  
[8] a) N. Zheng, Y. Xu, Q. Zhao, T. Xie, *Chem. Rev.* **2021**, 121, 1716; b) M. J. Webber, M. W. Tibbitt, *Nat. Rev. Mater.* **2022**, 7, 541; c) L. Leibler, M. Rubinstein, R. H. Colby, *Macromolecules* **1991**, 24, 4701; d) W. K. Zou, B. J. Jin, Y. Wu, H. J. Song, Y. W. Luo, F. H. Huang, J. Qian, Q. Zhao, T. Xie, *Sci. Adv.* **2020**, 6, aaz2362; e) Z. Fang, H. Mu, Z. Sun, K. Zhang, A. Zhang, J. Chen, N. Zheng, Q. Zhao, X. Yang, F. Liu, J. Wu, T. Xie, *Nature* **2024**, 631, 783.  
[9] a) A. M. Kloxin, A. M. Kasko, C. N. Salinas, K. S. Anseth, *Science* **2009**, 324, 59; b) Y. Gu, E. A. Alt, H. Wang, X. Li, A. P. Willard, J. A. Johnson, *Nature* **2018**, 560, 65.  
[10] Y. R. Li, B. Xue, J. H. Yang, J. L. Jiang, J. Liu, Y. Y. Zhou, J. S. Zhang, M. J. Wu, Y. Yuan, Z. S. Zhu, Z. J. Wang, Y. L. Chen, Y. Harabuchi, T. Nakajima, W. Wang, S. Maeda, J. P. Gong, Y. Cao, *Nat. Chem.* **2024**, 16, 446.  
[11] C. N. Zhu, C. Y. Li, H. Wang, W. Hong, F. H. Huang, Q. Zheng, Z. L. Wu, *Adv. Mater.* **2021**, 33, 2008057.  
[12] M. Q. Du, C. Li, *Adv. Mater.* **2024**, 36, 2408484.  
[13] S. L. Walden, P. H. D. Nguyen, H. K. Li, X. G. Liu, M. T. N. Le, L. X. Jun, C. Barner-Kowollik, V. X. Truong, *Nat. Commun.* **2023**, 14, 8298.  
[14] K. Z. Cheng, A. Chortos, J. A. Lewis, D. R. Clarke, *ACS Appl. Mater. Interfaces* **2022**, 14, 4552.  
[15] S. X. Wei, J. Smith-Jones, R. F. Lalisie, J. C. Hestenes, D. Y. Chen, S. P. O. Danielsen, R. C. Bell, E. M. Churchill, N. A. Munich, L. E. Marbella, O. Gutierrez, M. Rubinstein, A. Nelson, L. M. Campos, *Adv. Mater.* **2024**, 36, 2313961.  
[16] a) X. P. Li, R. Yu, Y. Y. He, Y. Zhang, X. Yang, X. J. Zhao, W. Huang, *ACS Macro. Lett.* **2019**, 8, 1511; b) P. Zhao, J. Xia, M. Cao, H. Xu, *ACS Macro. Lett.* **2020**, 9, 163.  
[17] a) F. Q. Fan, S. B. Ji, C. X. Sun, C. Liu, Y. Yu, Y. Fu, H. P. Xu, *Angew. Chem., Int. Ed.* **2018**, 57, 16426; b) C. Liu, J. H. Xia, S. B. Ji, Z. Y. Fan, H. P. Xu, *Chem. Commun.* **2019**, 55, 2813; c) X. Huang, S. Peng, L. Zheng, D. Zhuo, L. Wu, Z. Weng, *Adv. Mater.* **2023**, 35, 2304430.  
[18] J. J. Hernandez, S. P. Keyser, A. L. Dobson, A. S. Kuenstler, C. N. Bowman, *Macromolecules* **2024**, 57, 1426.  
[19] a) V. V. Zhang, J. Accardo, I. Kevlishvili, E. F. Woods, S. J. Chapman, C. T. Eckdahl, C. L. Stern, H. J. Kulik, J. A. Kalow, *Chem* **2023**, 9, 2298; b) D. J. Bischoff, T. Lee, K. S. Kang, J. Molineux, W. O. Parker, J. Pyun, M. E. Mackay, *Nat. Commun.* **2023**, 14, 7553.  
[20] H. Xiang, X. Li, B. Wu, S. Sun, P. Wu, *Adv. Mater.* **2023**, 35, 2209581.

- [21] a) K. H. Yu, Z. R. Feng, H. X. Du, A. Xin, K. H. Lee, K. T. Li, Y. P. Su, Q. M. Wang, N. X. Fang, C. Daraio, *Proc. Natl. Acad. Sci. USA* **2021**, *118*, 20165241118; b) A. K. Rylski, H. L. Cater, K. S. Mason, M. J. Allen, A. J. Arrowood, B. D. Freeman, G. E. Sanoja, Z. A. Page, *Science* **2022**, *378*, 211.
- [22] B. H. Liu, T. H. Yin, J. Y. Zhu, D. H. Zhao, H. H. Yu, S. X. Qu, W. Yang, *Proc. Natl. Acad. Sci. USA* **2023**, *120*, 2217781120.
- [23] J. D. Tang, J. Y. Li, J. J. Vlassak, Z. G. Suo, *Extreme Mech. Lett.* **2017**, *10*, 24.
- [24] a) M. Rottger, T. Domenech, R. van der Weegen, A. Breuillac, R. Nicolay, L. Leibler, *Science* **2017**, *356*, 62; b) S. Wang, Y. Hu, T. B. Kouznetsova, L. Sapir, D. Chen, A. Herzog-Arbeitman, J. A. Johnson, M. Rubinstein, S. L. Craig, *Science* **2023**, *380*, 1248.